Single-shot sonogram generation for femtosecond laser pulse diagnostics by use of two-photon absorption in a silicon CCD camera

Dmitriy Panasenko and Yeshaiahu Fainman

Department of Electrical and Computer Engineering, University of California, San Diego, 9500 Gilman Drive, La Jolla, California 92093-0407

Received March 6, 2002

We present an experimental technique capable of single-shot recording of an ultrashort laser pulse sonogram by use of two-photon absorption in a conventional silicon CCD camera. The quadratic spectral phase, introduced into a 100-fs pulse by a grating stretcher, was measured and found to be in good agreement with the analytically calculated value. The nonlinear response of silicon allows sonogram characterization in a wavelength range from 1 to 2 μm. © 2002 Optical Society of America

OCIS codes: 320.0320, 320.7100, 040.1520.

A commonly used method for complete characterization of the complex waveform of an ultrashort laser pulse is based on generation of its sonogram.[1,2] A sonogram $S(t, \omega)$ is a time–frequency representation of a complex amplitude signal, $p(t)$, that is formally equivalent to a spectrogram generated with the frequency-resolved optical gating technique.[3] As opposed to frequency-resolved optical gating, which uses a time-domain measurement, the sonogram is generated in the frequency domain:

$$S(t,\omega) = \left| \int \tilde{p}(\omega')\tilde{w}(\omega - \omega')\exp(i\omega' t)\mathrm{d}\omega' \right|^2, \qquad (1)$$

where $\tilde{p}(\omega) = \int p(t)\exp(-i\omega t)\mathrm{d}t$ is the Fourier amplitude of the signal and $\tilde{w}(\omega)$ is a filter function in the frequency domain. The sonogram displays the temporal position (or group delay) of different spectral components in the signal, permitting easy reconstruction of the signal's complex amplitude.[2] The sonogram can be generated with two-photon absorption in standard semiconductor photodetectors–an approach that allows detection of wide-spectral-bandwidth femtosecond pulses without the limitations imposed by the phase-matching process.[4–7] A sonogram detection system based on two-photon absorption in a GaAsP photodiode was reported recently.[6] This system uses mechanical scanning and allows real-time detection of the sonograms for high-repetition-rate (~100-MHz) mode-locked lasers. However, it is unlikely that this approach will support real-time operation for femtosecond laser systems with repetition frequency in the kilohertz range. In this Letter we report a single-shot femtosecond pulse correlation measurement[4,7]). We report, to the best of our knowledge for the first time, a single-shot sonogram generation technique based on two-photon absorption in a commercial silicon CCD array. The method is demonstrated with linearly chirped 100-fs pulses from an optical parametric amplifier at a wavelength of 1.4 μm.

Our experimental approach (see Fig. 1), based on the spectral decomposition of an ultrashort pulse, is a fast spectrometer consisting of a diffraction grating and a Fourier-transform lens. In commonly used spectrometers, the size of the input pupil is selected to be large to provide good spectral resolution. When an ultrashort pulse is spectrally decomposed in such a device, the time of flight of the ultrashort pulse through the input pupil determines the temporal duration of the spectrally decomposed wave in the focal plane of the lens. These considerations lead to the well-known time–frequency uncertainty: The better the spectral resolution of the device, the longer the time duration of the spectrally decomposed pulse, and therefore the lower the time resolution.[8] Thus, the spectral device with large input pupil gives no information about the relative temporal position of the different spectral components in the input ultrashort pulse. However, if we relinquish high spectral resolution and reduce the size of the input pupil, the temporal information becomes available and can be detected through a correlation measurement between each spectral component of the decomposed signal pulse and a time-domain reference pulse. This correlation measurement would provide us with a sonogram of the input ultrashort pulse.

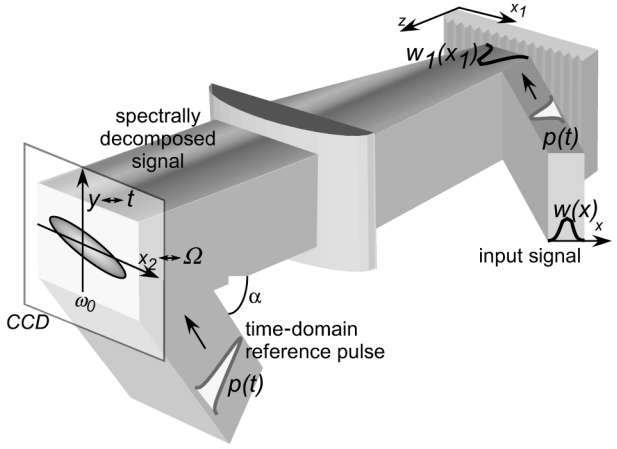

Fig. 1. Diagram of the experimental approach. The signal pulse is introduced into a low-resolution spectrometer dispersing optical frequency along the x_2 coordinate. A replica of the signal is used to produce the time reference along the y coordinate through nonlinear correlation with the spectrally decomposed signal on the CCD camera.

0146-9592/02/161475-03$15.00/0

Our experimental approach is illustrated schematically in Fig. 1. An ultrashort pulse with complex amplitude $p(t)$ at a carrier frequency ω_0 with transverse spatial mode $w(x)$ is diffracted by the grating and then Fourier transformed by a cylindrical lens in the x direction. The field in the back focal plane of the lens is described by[9]

$$E_F(t,x') \propto \int \tilde{w}_1\left(\frac{\omega_0}{cf}x_2 - \frac{2\pi}{\omega_0 d}\Omega\right)\tilde{p}(\Omega)\exp(j\Omega t)\mathrm{d}\Omega\,, \tag{2}$$

where $\tilde{w}_1$ is a Fourier transform of the spatial mode distribution $w_1(x_1)$ on the surface of the grating, $\Omega = \omega - \omega_0$ is the frequency shift from the carrier ω_0, c is the speed of light in vacuum, f is the focal length of the cylindrical lens, d is the grating period, and x_2 is the transverse spatial coordinates in the spatial Fourier-transform plane (see Fig. 1). The system described by expression (2) implements a spectral filter with transfer function $\tilde{w}_1(\omega_0 x_2/cf - 2\pi\Omega/\omega_0 d)$. The filter bandwidth is determined by the size of the spatial mode on the input grating (see Fig. 2). Next, we introduce a replica of the input signal pulse to establish a time reference (see Fig. 1). The temporal reference beam is introduced at an angle α relative to the x–z plane, defining the time axis in the y direction. The reference signal interacts with the spectrally decomposed wave on the surface of the CCD array, producing a cross-correlation function through the two-photon absorption process. Assuming that the duration of the reference is much less than that of the spectrally decomposed field, we approximate the reference pulse by a δ function:

$$E_{\mathrm{ref}} \propto \delta[t - y\,\sin(\alpha)/c]\exp(j\omega_0 t)\,, \tag{3}$$

yielding the intensity correlation between the fields of expressions (2) and (3):

$$I(y,x_2) \propto \left|\int \tilde{W}_1\left(\frac{\omega_0}{cf}x_2 - \frac{2\pi}{\omega_0 d}\Omega\right)\tilde{p}(\Omega) \times \exp[\,j\Omega y\,\sin(\alpha)/c]d\Omega\right|^2. \tag{4}$$

At every spatial coordinate x_2, the position of the correlation peak along the y axis defines the temporal position of the corresponding spectral component $\Omega = (\omega_0^2 d/2\pi cf)x_2$; the set of these correlation functions forms a sonogram.

In the experiments we used a spectral device consisting of a 300-line/mm diffraction grating and a cylindrical lens with a focal distance of 250 mm. A variable rectangular slit was used to control the input pupil of the spectrometer. The slit was telecentrically imaged onto the grating surface in the x direction by use of a cylindrical lens telescope with a 1:3 demagnification factor. The demagnification allowed us to increase the spatial filter power throughput. The size of the spatial mode on the grating was ~150 μm, corresponding to approximately one-quarter of the pulse bandwidth. We use an optical parametric amplifier that produces almost-transform-limited 100-fs pulses with an energy of ~10 μJ at a wavelength of 1.4 μm. The camera used for sonogram generation was a silicon CCD Pulnix TM-7 with 10-μm pixel size. The bandgap of silicon corresponds to a wavelength of 1.06 μm, and therefore we observed quadratic response at 1.4 μm.

To test our technique, we used a grating pair to synthesize a linearly chirped ultrashort pulse. An image corresponding to the generated sonogram is shown in Fig. 3. It can be easily deduced from expression (3) that the sonogram rotation angle for the case of linear chirp [$\tilde{p}(\Omega) \sim \exp(ia\Omega^2)$] is approximately $a\omega_0^2 d/\pi f\,\sin(\alpha)$, where a is the amount of the quadratic phase in the frequency domain. With our experimental setup parameters, stretching a 100-fs pulse in time approximately twice caused sonogram rotation by ~10°. The fringe structure inside the sonogram that appears because of the interferometric nature of the generated cross correlation does not affect our measurements, as it can be easily filtered out digitally.

As each of the interacting beams generates its own two-photon absorption current in the CCD, our measurement is not background free. It is well known[4,10] that the maximum signal-to-background

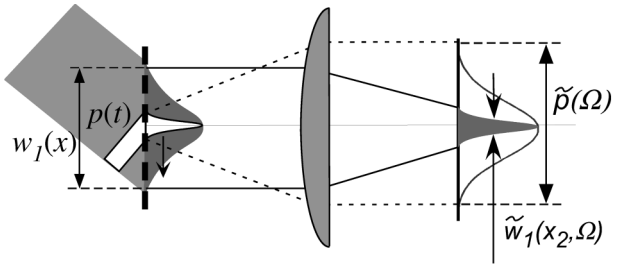

Fig. 2. Illustration of the filtering of the ultrashort pulse spectrum by the spatial mode in the spectral device. The ultrashort pulse and the spatial mode on the surface of the grating are indicated by the white and gray Gaussians, respectively. The lens performs a Fourier transform on both the temporal and the spatial parts of the signal generating the filter function as described by expression (2).

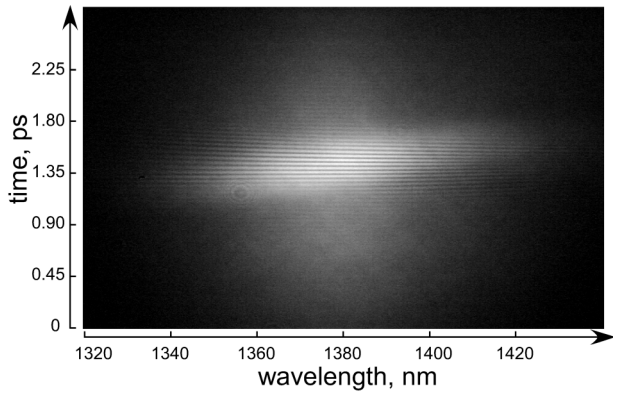

Fig. 3. CCD snapshot of the sonogram of a linearly chirped pulse. The fringes inside the sonogram are due to the interferometric nature of the generated correlation.

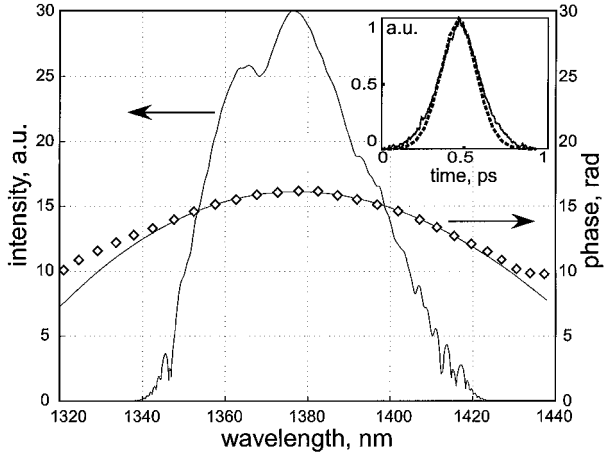

Fig. 4. Spectrum of the signal together with the spectral phase (diamonds) extracted from the sonogram of Fig. 3. The quadratic spectral phase calculated from the grating stretcher geometry is shown for comparison (solid curve). Inset, autocorrelation of the pulse on the output of the grating stretcher obtained with moving delay-line correlator (solid curve) and autocorrelation (dashed curve) calculated from the pulse shape extracted from the sonogram.

ratio for intensity autocorrelation measurements, which occurs when the power is split equally between the two interacting channels, is 3 to 1. It should be noted, however, that the signal-to-background ratio for a cross-correlation measurement depends on both the relative intensity of the interacting beams and the relative pulse width. To obtain maximum signal-to-background ratio in the sonogram measurement, one should optimize the relative intensity for each bandwidth of the filter to provide equal integral intensity of the squared fields $\int |E^2|^2 \mathrm{d}t$ in both channels. We estimated numerically the signal-to-background ratio for cross-correlation measurement by assuming a Gaussian pulse shape. When one of the pulses is two or three times wider than the other, the maximum signal-to-background ratio drops to 2.8:1 and 2.5:1, respectively. In our experiments (after filtering out the fringe structure) we observed a signal-to-background ratio of approximately 2:1, somewhat lower than expected, which is due in part to nonoptimized power balance and imperfections of the spatial mode.[10]

The phase reconstruction from the sonogram was described in detail elsewhere.[2,11] The group delay, $\mathrm{d}\tilde{\varphi}(\omega)/\mathrm{d}\omega$, of the signal is determined from the relative temporal position of the correlation peak for each spectral component. The spectral phase $\tilde{\varphi}(\omega)$ is then obtained by integration. Note that for signals with an ill-defined group-delay function an iterative reconstruction procedure can be utilized.[12,13]

Figure 4 shows the spectral phase extracted from the sonogram obtained with the experimental system of Fig. 1. The spectrum was measured separately by means of blocking the reference pulse. This allowed us to maintain higher power density of the reference pulse, as we only have to expand its spatial mode in the y direction to provide uniform mode cross section for the measurement of the correlation peak position. The quadratic phase introduced by the grating stretcher can be calculated analytically.[14] Figure 4 shows good agreement between the calculated and the measured phase. We believe that the small deviations in the measured phase from the quadratic function behavior (see Fig. 4) are primarily due to decreased signal-to-ratio near the edges of the spectrum.

In conclusion, we present a novel experimental technique for single-shot detection of the sonogram for femtosecond laser pulses, exploiting two-photon absorption in a commercial silicon CCD camera. The technique employs a fast spectrometer operating at low resolution, thereby permitting detection of the temporal position of the spectral components in the input signal. With a standard silicon CCD array this technique is applicable to the wavelength range 1.1–2.2 μm. Other wavelengths can be analyzed by use of detector arrays made from different materials or by use of higher-order nonlinear optical processes.[15]

This work was supported by the National Science Foundation, the Defense Advanced Research Projects Agency, and Applied Micro Circuits Corporation. The authors are grateful to Y. Mazurenko for fruitful discussions. D. Panasenko gratefully acknowledges the support of the Fannie and John Hertz Foundation. His e-mail address is dpanasen@ece.ucsd.edu.

References

1. J. L. A. Chilla and O. E. Martinez, Opt. Lett. **16,** 39 (1991).
2. J.-K. Rhee, T. S. Sosnowski, A.-C. Tien, and T. B. Norris, J. Opt. Soc. Am. B **13,** 1780 (1996).
3. D. J. Kane and R. Trebino, Opt. Lett. **18,** 823 (1993).
4. Y. Takagi, T. Kobayashi, K. Yoshihara, and S. Imamura, Opt. Lett. **17,** 658 (1992).
5. D. T. Reid, W. Sibbett, J. M. Dudley, L. P. Barry, B. Thomsen, and J. D. Harvey, Appl. Opt. **37,** 8142 (1998).
6. I. G. Cormack, W. Sibbett, and D. T. Reid, J. Opt. Soc. Am. B **18,** 1377 (2001).
7. D. Panasenko and Y. Fainman, Appl. Opt. **41,** 3748 (2002).
8. E. B. Treacy, J. Appl. Phys. **42,** 3848 (1971).
9. M. B. Danailov and I. P. Christov, J. Mod. Opt. **36,** 725 (1989).
10. H. P. Weber and H. G. Danielmeyer, Phys. Rev. A **2,** 2074 (1970).
11. J. L. A. Chilla and O. E. Martinez, IEEE J. Quantum Electron. **27,** 1228 (1991).
12. V. Wong and I. A. Walmsley, J. Opt. Soc. Am. B **14,** 944 (1997).
13. D. T. Reid, IEEE J. Quantum Electron. **35,** 1584 (1999).
14. E. B. Treacy, IEEE J. Quantum Electron. **QE-5,** 454 (1969).
15. K. A. Briggman, L. J. Richter, and J. C. Stephenson, Opt. Lett. **26,** 238 (2001).